P2X7 receptor antagonism suppresses epileptiform-like activity in an inflammation-primed human iPSC-derived neuron model of drug-resistant epilepsy

Jaideep Kesavan[1], Klaus Dinkel[2], Michael Hamacher[3], Jochen Prehn[1], David Henshall[1], and Tobias Engel[1]

[1]Royal College of Surgeons in Ireland
[2]Lead Discovery Center GmbH
[3]Affectis Pharmaceuticals AG

September 01, 2024

Abstract

Background and Purpose Neuroinflammation is increasingly recognized to contribute to drug-resistant epilepsy. Activation of the ATP-gated P2X7 receptor (P2X7R) has emerged as an important upstream mechanism and increased P2X7R expression is present in the seizure focus in rodent models and patients. Pharmacologic antagonism of the P2X7R can attenuate seizures in rodents but this has not been explored in human neuronal networks. Experimental Approach Human neurons were differentiated from two induced pluripotent stem cell (hiPSC) lines. P2X7R function on neurons was assessed via P2X7R agonist BzATP-evoked calcium transients. Acute or chronic in vitro models of epileptiform-like events were generated by exposure of hiPSC cultures to the GABAA receptor antagonist picrotoxin or a cocktail of picrotoxin and neuroinflammatory agents with or without the presence of P2X7R antagonists. Epileptiform-like activity was measured via single cell patch-clamp recordings. Key Results BzATP application (300 μM) resulted in increased calcium influx in hiPSC-derived neurons which was blocked by the P2X7R antagonists JNJ-47965567 (100 nM) and AFC-5128 (30 nM). Single-cell patch-clamp recordings showed that, while treatment with AFC-5128 did not reduce epileptiform-like activity triggered by picrotoxin alone, AFC-5128 reduced the severity of epileptiform-like activity under inflammatory conditions. Notably, epileptiform-like events in the inflammation-primed picrotoxin model were refractory to the anti-seizure medication carbamazepine alone but were reduced by the co-application of carbamazepine with AFC-5128. Conclusion and Implications Our findings demonstrate anti-seizure effects of targeting the P2X7R in a human neuronal network model of epilepsy and suggest P2X7R-based treatments may be an effective add-on therapy for controlling drug-resistant seizures.

Title: P2X7 receptor antagonism suppresses epileptiform-like activity in an inflammation-primed human iPSC-derived neuron model of drug-resistant epilepsy

Running title : P2X7R antagonism reduces epileptiform-like activity in human iPSC neurons

Authors: Jaideep Kesavan[1,2], Klaus Dinkel[3], Michael Hamacher[4], Jochen H. M. Prehn[1,2], David C. Henshall[1,2]and Tobias Engel[1,2]*

Affiliations :

[1] Department of Physiology & Medical Physics, RCSI University of Medicine & Health Sciences, Dublin, D02 YN77, Ireland

[2] **FutureNeuro, SFI Research Centre for Chronic and Rare Neurological Diseases** , RCSI University of Medicine and Health Sciences, Dublin, D02 YN77, Ireland

[3] Lead Discovery Center GmbH, Otto-Hahn-Straße 15, 44227 Dortmund, Germany

[4] Affectis Pharmaceuticals AG, Otto-Hahn-Straße 15, 44227 Dortmund, Germany

**Correspondence:* Tobias Engel, Ph.D., Department of Physiology & Medical Physics, RCSI University of Medicine & Health Sciences, Dublin, D02 YN77, Ireland

Tel: +35314025199, Fax: +35314022447, Email:*tengel@rcsi.ie*

Manuscript details: Page numbers: 33; Figure numbers: 5; Tables: 2; Abstract: 250 words, Introduction: 620 words; Results: 2283; Discussion: 885 words; References: 52

Abstract

Background and Purpose

Neuroinflammation is increasingly recognized to contribute to drug-resistant epilepsy. Activation of the ATP-gated P2X7 receptor (P2X7R) has emerged as an important upstream mechanism and increased P2X7R expression is present in the seizure focus in rodent models and patients. Pharmacologic antagonism of the P2X7R can attenuate seizures in rodents but this has not been explored in human neuronal networks.

Experimental Approach

Human neurons were differentiated from two induced pluripotent stem cell (hiPSC) lines. P2X7R function on neurons was assessed via P2X7R agonist BzATP-evoked calcium transients. Acute or chronic *in vitro* models of epileptiform-like events were generated by exposure of hiPSC cultures to the $GABA_A$ receptor antagonist picrotoxin or a cocktail of picrotoxin and neuroinflammatory agents with or without the presence of P2X7R antagonists. Epileptiform-like activity was measured via single cell patch-clamp recordings.

Key Results

BzATP application (300 μM) resulted in increased calcium influx in hiPSC-derived neurons which was blocked by the P2X7R antagonists JNJ-47965567 (100 nM) and AFC-5128 (30 nM). Single-cell patch-clamp recordings showed that, while treatment with **AFC** -5128 did not reduce epileptiform-like activity triggered by picrotoxin alone,**AFC** -5128 reduced the severity of epileptiform-like activity under inflammatory conditions. Notably, epileptiform-like events in the inflammation-primed picrotoxin model were refractory to the anti-seizure medication carbamazepine alone but were reduced by the co-application of carbamazepine with **AFC** -5128.

Conclusion and Implications

Our findings demonstrate anti-seizure effects of targeting the P2X7R in a human neuronal network model of epilepsy and suggest P2X7R-based treatments may be an effective add-on therapy for controlling drug-resistant seizures.

Keywords

Human derived pluripotent stem cell-(hiPSC)-derived neurons, In vitro model of drug-resistant seizures, P2X7 receptor, ATP, Inflammation

Abbreviations

ASM, anti-seizure medication; C1q, complement component 1q; DAMP, damage-activated pattern; BzATP, 2',3'-O-(4-benzoylbenzoyl)-ATP; eATP, extracellular ATP; **ΓΑΒΑ, γ-αμινοβυτψρις αςιδ·** hiPSCs, human induced pluripotent stem cells; IBI, inter-burst-intervals; IL, Interleukin; P2X7R, purinergic P2X7 receptor; **KDE, Kernel density estimation;** pNSCs, primitive neural stem cells; PTX, picrotoxin; TNF-α, tumour necrosis factor-α

Bullet point summary:

What is already known

P2X7R expression is increased in epileptogenic tissue in the brains of animal models of epilepsy and epilepsy patients.

P2X7R antagonism can attenuate seizures in animal models.

What this study adds

P2X7Rs are expressed and functional on hiPSC-derived neurons.

P2X7R antagonism reduces drug-refractory seizures in a human epilepsy cell model system under inflammatory conditions.

What is the clinical significance

The findings suggest P2X7R antagonism could be an add-on therapy for patients with drug-refractory epilepsy.

1. Introduction

Epilepsy is a common brain disease characterized by spontaneous recurrent seizures that affects up to 70 million people worldwide (Thijs et al., 2019). Epilepsy can be caused by a variety of factors including inherited and de novo gene mutations or can be acquired as a result of a brain injury (Pitkanen et al., 2015; Steinlein, 2008). While there are over 30 approved anti-seizure medications (ASMs) in clinical use, pharmacoresistance remains as high as 30%, a rate that has not changed in decades (Klein et al., 2024). Moreover, ASMs have shown no apparent impact on disease progression and can cause serious side effects (*e.g* ., dizziness, headaches) (Perucca et al., 2023), highlighting the need for novel therapies.

The cell and molecular hallmarks of neuroinflammation are a common finding in brain samples from patients who underwent neurosurgical resection of seizure-generating tissue. Accordingly, there is interest in therapeutic targeting of neuroinflammatory pathways such as interleukin-1β (IL-1β) for seizure control and possibly disease modification (Aronica et al., 2017; Devinsky et al., 2013; Vezzani et al., 2011). Extracellularly released adenosine triphosphate (eATP) functions as a damage-activated molecular pattern (DAMP), mediating pro- and anti-inflammatory effects via ionotropic P2X and metabotropic P2Y receptors (Andrejew et al., 2020; Beamer et al., 2021). Among these, the P2X7 receptor (P2X7R) has attracted particular attention (Beamer et al., 2017; Engel et al., 2021). Activation of the P2X7R requires high amounts of eATP, limiting its function mainly to pathophysiologic circumstances, and results in opening of a non-selective cationic channel permeable to Na^+, K^+ and Ca^{2+}, leading to the later release of IL-1β. The receptor is normally expressed at low levels in the brain, in particular on microglia and oligodendrocytes (Alves et al., 2024; Illes et al., 2017; Kaczmarek-Hajek et al., 2018). P2X7R expression increases in the brain in experimental models of epilepsy and is elevated within the hippocampus from patients with treatment-resistant epilepsy (Alves et al., 2024; Dona et al., 2009; Engel et al., 2012; Jimenez-Pacheco et al., 2016; Morgan et al., 2020). P2X7Rs have been implicated in a variety of pathological processes relevant to epilepsy including increased permeability of the blood brain-barrier (BBB), altered neurotransmitter release, cell death and neuroinflammation (Andrejew et al., 2020; Klein et al., 2018; Sperlagh et al., 2014).

Functional studies indicate that targeting the P2X7R can attenuate seizures. For example, P2X7R antagonists, such as AFC-5128 and JNJ-47965567, have been shown to reduce the severity of evoked and spontaneous seizures in mice (Amhaoul et al., 2016; Amorim et al., 2017; Engel et al., 2012; Jimenez-Mateos et al., 2015; Jimenez-Pacheco et al., 2016; Jimenez-Pacheco et al., 2013; Mamad et al., 2023; Rozmer et al., 2017). It is unclear, however, whether these therapeutic effects will translate to humans as there are

sequence and functional differences between the rodent and human P2X7R and controversy over whether neurons express functional P2X7Rs (Illes et al., 2017).

Human induced pluripotent stem cells (hiPSCs) represent invaluable human model systems to test the effects of new drugs on human cells, thereby advancing treatments further towards a clinical application (Autar et al., 2022; Jones et al., 2016; Rivetti di Val Cervo et al., 2021). While P2X7Rs have been shown to be present on several hiPSCs-induced cell lines including microglia, astrocytes and neurons (Francistiova et al., 2021; Kesavan et al., 2023), whether P2X7R signaling contributes to hyperexcitable networks using hiPSCs has not been investigated. Here, we show, using an in vitro model of epileptiform-like events in hiPSCs-derived neurons, that P2X7R antagonism can reduce epileptiform activity but only in the context of a primed inflammatory state. We further show that P2X7R antagonism has a synergistic effect when co-applied with a conventional ASM, providing support for the use of P2X7R-based drugs as stand-alone or adjunctive treatments for pharmacoresistant epilepsy.

2. Methods

2.1. Culture and differentiation of hiPSCs

All hiPSC-related work was approved by the RCSI Research Ethics Committee (REC202302020). hiPSC line HPSI0114i-eipl_1 (ECACC 77650081; Culture Collections, Public Health England, UK) was made by reprogramming with a non-integrating virus from skin fibroblasts from a healthy individual at passage 32. Cells were maintained under feeder-free conditions on vitronectin (STEMCELL Technologies, British Columbia, Canada)-coated 6-well plates in E8 medium (Thermo Fisher Scientific, Massachusetts, USA). hiPSCs were dissociated by using 0.5 mM EDTA for 2 min at 37°C, and reseeded at the density of 1 x 10^4 cells per cm^2. For the neural induction of hiPSCs, approximately 24 h after splitting, culture medium was switched to Gibco PSC Neural Induction Medium (Thermo Fisher Scientific, Massachusetts, U.S.A.) containing Neurobasal medium and Gibco PSC neural induction supplement. Neural induction medium was changed every other day from day 0 to day 4 of neural induction and every day thereafter. At day 10 of neural induction, primitive neural stem cells (pNSCs) were dissociated with Accutase (Thermo Fisher Scientific, Massachusetts, USA) and plated on Geltrex-coated dishes at a density of 1 x 10^5 cells per cm^2 in NSC expansion medium containing 50% Neurobasal medium, 50% Advanced DMEM/F12, and 1% neural induction supplement (Thermo Fisher Scientific, Massachusetts, U.S.A.). pNSCs were passaged on the 4^{th}day at a 1:3 split ratio to derive NSCs. For the differentiation of neurons, NSCs were plated on Geltrex-coated coverslips or on a monolayer of human primary glia at a density of 5 x 10^4 cells per cm^2 in neuronal differentiation medium consisting of neurobasal medium and DMEM-F12 (1:1), with 2% B-27 supplement, 1% N2 supplement, 1% L-glutamine, 1% nonessential animal acids, 20 ng/ml brain-derived neurotrophic factor (BDNF), 20 ng/ml glial cell-derived neurotrophic factor (GDNF) (all from Thermo Fisher Scientific, Massachusetts, USA), 100 ng/mL cAMP, 100 µM L-ascorbic acid and penicillin/streptomycin (all from Merck, Missouri, United States). The culture medium was changed every 2-3 days. Neurons which were differentiated from hiPSC-derived neural progenitors, hereafter referred as hiPSC line 2, were obtained from Roche Pharmaceuticals (Lau et al., 2024).

2.2. Immunocytochemistry

Neurons cultured on coverslips were fixed with a combination of acetic acid (6.71%) and ethanol (62.5%) for 15 min. After 3 washes in phosphate buffered saline, cells were permeabilized with 0.1% Triton for 20 min and blocked in 1% BSA for 30 min. Cells were incubated at 4°C overnight in primary antibody diluted in 1% BSA. Cells were then incubated in secondary antibody diluted in 1% BSA for 1 h at room temperature. The following primary antibodies were used: mouse anti-β-tubulin III as a marker for neuron-specific cytoskeletal proteins (Biolegend, San Diego, CA, dilution 1:500) and rabbit anti-P2X7R (Alomone Labs, Jerusalem, Israel, dilution 1:200) or rabbit anti-P2X7R (Synaptic Systems, Göttingen, Germany, dilution 1:200) as markers for P2X7R. The respective secondary antibodies were conjugated to Alexa Fluor-488 or Alexa Fluor-594 (Thermo Fisher Scientific, Massachusetts, USA) and used at a dilution of 1:1000. Coverslips were mounted and images were acquired using a Leica DM4000B fluorescence microscope.

2.3. Drug application

Stock solutions of BzATP (Alomone Labs, Jerusalem, Israel), ATP (Merck, Missouri, United States), AFC-5128 (Beamer et al., 2022) and JNJ-47965567 (Alomone Labs, Jerusalem, Israel) were diluted and applied in HEPES-buffered extracellular solution. The drug solutions were delivered to the recorded cells by a valve-controlled fast multibarrel superfusion system with a common outlet approximately 350 µm in diameter (Automate Scientific, California, USA). The application tip was routinely positioned approximately 1 mm away from and 50 µm above the surface of the recorded cells. A computer connected to Digidata 1550B controlled the onset and duration of each drug application. The drugs were used at the following final concentration: BzATP and ATP (300 µM), AFC-5128 (30 nM) and JNJ-47965567 (100 nM).

2.4. Calcium Imaging

For calcium imaging of BzATP-evoked responses, neurons, differentiated on Geltrex-coated coverslips without human primary glia, were loaded with Cal-520 (AAT Bioquest, California, USA) by incubation with the acetoxymethyl (AM) ester form of the dye at a final concentration of 2 µM in culture media without serum. The dyes were prepared as 5 mM stock solution in dimethyl sulfoxide (DMSO) and kept frozen at -20°C and diluted on the day of use. After 45 min, cells were washed several times with dye-free HEPES-buffered saline solution and transferred to an imaging chamber on a microscope (Zeiss Axio Examiner, Jena, Germany) equipped with a Zeiss 40x water immersion objective. Zen Blue imaging software (Carl Zeiss, Jena, Germany) was used for hardware control and image acquisition, and image analysis was performed using ImageJ (NIH, Maryland, USA). All imaging experiments were performed at 34°C in a low divalent cation-containing bath solution with the composition (in mM): 135 NaCl, 3 KCl, 0.5 $CaCl_2$, 0.1 $MgCl_2$, 10 HEPES and 10 glucose (pH 7.2; osmolality 290-300 mmol/kg). Images were acquired at 4 Hz. Background fluorescence was measured from the cell-free area outside the soma of interest in each frame of every time series. Region of interests (ROIs) were manually drawn around the soma and baseline fluorescence intensity (F0) was determined by averaging 24 frames preceding the cell's exposure to BzATP or ATP and the time course of normalized fractional dye fluorescence [ΔF/F0] was obtained, where ΔF equals F(t) - F0.

2.5. Induction of acute or chronic epileptiform-like activity

Neurons plated on human primary glia was used for the induction of acute or chronic epileptiform-like activity. Acute epileptiform-like activity was induced by exposure to the chemical convulsant picrotoxin (100 µM) for 10 min. To induce chronic epileptiform-like activity, the cultures were exposed to picrotoxin (100 µM) for 7 to 12 days where a chronic epileptiform-like activity with neuroinflammation was induced by treating the cultures with a cocktail of picrotoxin (100 µM), tumour necrosis factor-α (TNF-α) (30 ng/ml), IL-1α (3 ng/ml), IL-1β (3 ng/ml) and complement component 1q (C1q) (400 ng/ml) for 7 to 12 days**(Hyvarinen et al., 2019; Stoberl et al., 2023)** .

2.6. Burst detection and analysis

Loose patch-clamp experiments were carried out with a Multiclamp 700 B amplifier (Molecular Devices, California, USA) which was interfaced by an A/D-converter (Digidata 1550B, Molecular Devices, California, USA) to a PC running pClamp software (Version 11, Molecular Devices, California, USA). The signals were low-pass filtered at 2 kHz and sampled at 10 kHz. Pipette electrodes (G150T-4, Harvard Apparatus, Massachusetts, USA) were fabricated using a vertical puller (Narishige PC-100, Tokyo, Japan). All recordings were performed at 34°C in a bath solution containing (in mM): 135 NaCl, 3 KCl, 2 $CaCl_2$, 1 $MgCl_2$, 10 HEPES and 10 glucose (pH 7.2; osmolality 290-300 mmol/kg). Spontaneous action potential firing and bursts were detected in loose-patch configuration with patch pipettes filled with the bath solution. A spike was counted when the signal recorded in loose patch configuration exceeded a threshold of $\pm 5\ \sigma$, where σ was the standard deviation of the baseline noise during quiescent periods. The following parameters were used for burst detection: maximum interval to start burst was set to 100 ms, maximum continuing in-burst interval was set to 5000 ms, and minimum number of spikes in a burst was set to 5.

2.7. Statistical analysis

The manuscript complies with BJP's recommendations and requirements on experimental design and analysis. All experiments were designed to generate groups of equal size, using randomisation and blinded analysis. All statistical analyses were performed with GraphPad Prism 9 software (GraphPad Software, San Diego, CA, USA) and are described in Figure legends. Initially, all datasets were tested for normality using the Shapiro-Wilk test. For datasets failing normality, Mann-Whitney test (two-tailed) was performed. For multiple comparisons, repeated-measures ANOVA and Tukey's Post hoc tests were performed. Non-parametric**Kolmogorov-Smirnov test was used to test for one-dimensional probability distribution.** Data are expressed as mean ± SEM.$p < 0.05$ was considered statistically significant.

3. Results

3.1. Functional expression of P2X7Rs in hiPSC-derived neurons

In order to assess the functional expression of P2X7Rs and if targeting of these receptors reduces hyperexcitability in a human brain-relevant cellular model, we differentiated neurons from two hiPSC lines (Kesavan et al., 2023).

As a first approach, immunocytochemistry was performed on cells at 18-22 days after plating NSCs using two different P2X7R antibodies and the neuronal marker β-III tubulin. Of note, while the β-III tubulin antibody produced a more diffuse staining, the P2X7R antibodies showed the expected punctate staining in the neuronal soma and along the processes, demonstrating the presence of P2X7Rs on hiPSC-derived neuronal soma and processes (**Figure 1a-c**).

To complement the immunocytochemistry findings, we next sought to assess whether these human neurons respond to the application of P2X7R-stimulating agonists. Previous studies have shown that the activation of the P2X7R requires high (mM range) concentrations of ATP. The P2X7R is, however, 10-30 times more sensitive to the ATP analog and non-selective P2X7R agonist, 2',3'-O-(4-benzoylbenzoyl)-ATP (BzATP) (Donnelly-Roberts et al., 2009). To assess the functional expression of P2X7Rs, hiPSC line 1-derived neurons grown on coverslips without glial monolayer were loaded with 2 μM Cal-520 AM calcium-sensitive fluorescent dye to eliminate unspecific fluorescence from glia. The application of the P2X7R agonist BzATP (300 μM) resulted in a discernable increase in calcium fluorescence in hiPSc line 1-derived neurons (**Figure 2a**). Fluorescence rose quickly in response to a pulse of 300 μM BzATP for 5 s signifying a persistent rise in $[Ca^{2+}]$i during constant agonist exposure. In contrast, when the cells were pre-incubated with the P2X7R antagonist AFC-5128 (Fischer et al., 2016; Kesavan et al., 2023) (30 nM) pulse ejection of 300 μM BzATP and 30 nM AFC-5128, changes in $[Ca^{2+}]_i$ were strongly reduced (BzATP 0.0819 ± 0.0060, BzATP and AFC-5128 0.0127 ± 0.0050; $p < 0.0001$). The peak amplitude of the individual ΔF/F0 traces upon BzATP application was reduced when stimulated in the presence of AFC-5128 (BzATP 0.2086 ± 0.0362, BzATP and AFC-5128 0.0975 ± 0.024;$p < 0.0001$) (**Figure 2b**). Similar results were evident when the area under ΔF/F0 curve (AUC) of individual ΔF/F0 traces were compared (BzATP 2.170 ± 0.2276, BzATP and AFC-5128 0.5178 ± 0.1307;$p < 0.0001$) (**Figure 2c**), suggesting BzATP-evoked responses are mediated mainly via the P2X7R.

To further confirm the functional expression of P2X7Rs, we repeated the BzATP application in the presence of another highly-specific P2X7R antagonist, JNJ-47965567. Similar to AFC-5128, BzATP-evoked $[Ca^{2+}]_i$ signals were also reduced in the presence of a second P2X7R antagonist JNJ-47965567 (BzATP 0.1089 ± 0.0134, BzATP and JNJ-47965567 0.0209 ± 0.0004; $p < 0.000$) (**Figure 2d**). The peak amplitude of the individual ΔF/F0 traces upon BzATP application was reduced when stimulated in the presence of JNJ-47965567 (BzATP 0.6528 ± 0.0428, BzATP and JNJ-47965567 0.0460 ± 0.0064, mean ± SEM; $p < 0.0001$) (**Figure 2e**). As before, similar results were evident when the area under ΔF/F0 curve of individual ΔF/F0 traces were compared (BzATP 2.808 ± 0.1811, BzATP and JNJ-47965567 0.0777 ± 0.0114;$p < 0.0001$) (**Figure 2f**).

We further confirmed the expression of P2X7Rs using hiPSC line 2-derived neurons. Bz-ATP evoked Ca^{2+} influx was also blocked by AFC-5128 (BzATP 0.0592 ± 0.0038, BzATP and AFC-5128 0.0035 ± 0.0011) (**Figure 2g**). The peak amplitude of the individual ΔF/F0 traces upon BzATP application was reduced when stimulated in the presence of AFC-5128 (BzATP 0.1359 ± 0.0233, BzATP and AFC-5128 0.0674

± 0.0086; $p < 0.0111$) (**Figure 2h)** . Similar results were obtained when the area under ΔF/F0 curve of individual ΔF/F0 traces were compared (BzATP 1.367 ± 0.2385, BzATP and JNJ-47965567 0.4862 ± 0.0849; $p = 0.0007$) (**Figure 2i**). BzATP-evoked Ca^{2+} influx was also blocked by JNJ-47965567 (BzATP 0.0241 ± 0.0035, BzATP and JNJ-47965567 0.0018 ± 0.0008; $p < 0.0001$) (**Figure 2j**). The peak amplitude of the individual ΔF/F0 traces upon BzATP application was reduced when stimulated in the presence of JNJ-47965567 (BzATP 0.2110 ± 0.0299, BzATP and JNJ-47965567 0.0631 ± 0.0115; $p = 0.0002$) (**Figure 2k**). A comparison of area under ΔF/F0 curve of individual ΔF/F0 traces reveals a significant reduction in the presence of JNJ-47965567 (BzATP 1.584 ± 0.2567, BzATP and JNJ-47965567 0.5119 ± 0.1265; $p = 0.0002$) (**Figure 2l**). These results demonstrate the functional expression of P2X7Rs in two lines of hiPSC-derived neurons.

3.2. Antagonism of P2X7Rs alleviates PTX-induced chronic epileptiform-like events under inflammatory conditions

Pharmacological targeting of P2X7Rs have repeatedly been proven effective in rodent models of epilepsy (Engel et al., 2012; Jimenez-Pacheco et al., 2016; Jimenez-Pacheco et al., 2013; Mamad et al., 2023). The effects of P2X7R antagonism on hyperexcitability in a human neuronal network has, however, not been reported to date. For this, we first developed an in vitro model consisting of hiPSC-derived neurons differentiated on human primary astrocytes. When co-cultured with astrocytes, functional maturation of hiPSC-derived neurons has been shown to be improved (Hedegaard et al., 2020; Johnson et al., 2007).**Ηερε, νετωορκ περτυρβατιονς λεαδινγ το επιλεπτιφορμ-λικε βυρστς ωερε ινδυςεδ ια τηε αππλιςατιον οφ ΠΤΞ (100 μM), α νον-ςομπετιτιε ανταγονιστ οφ ινηιβιτορψ γ-αμινοβυτψρις αςιδ (ΓΑΒA_A) ρεςεπτορς (Φιγυρε 3α, β). Λοοσε πατςη-ςλαμπ εξπεριμεντς ωερε περφορμεδ το ασσεσς νετωορκ εξςιτα-βιλιτψ. Ας δεπιςτεδ βψ εξεμπλαρψ τραςες ανδ χυαντιφιςατιονς, λοοσε πατςη-ςλαμπ εξπεριμεντς σηοωεδ τηατ τρεατμεντ ωιτη ΠΤΞ φορ 10 μιν ινςρεασεδ τηε βυρστ φρε-χυενςψ φρομ 0.0558 ± 0.0146 Ηζ ατ βασελινε το 0.0925 ± 0.0149 Ηζ· π = 0.0358) ποστ-τρεατμεντ (Φιγυρε 3ς).** Similarly, calcium imaging experiments using Cal-520 loaded neurons also revealed PTX induced an increase in network activity and synchronisation, hallmarks of seizures (**Figure 3d, e**).

We next assessed the effect of P2X7R antagonism in this model (Figure 4a). Comparison of burst parameters during PTX application vs. co-application of PTX and AFC-5128 revealed no significant difference in burst frequency ([F(2,11) = 1.79; $p = 0.2053$)]: baseline 0.0800 ± 0.0277, PTX 0.1421 ± 0.044, PTX and AFC-5128 0.0995 ± 0.0227 Hz), number of spikes in burst (([F(2,11) = 1.79; $p = 0.2053$)]: baseline 19.65 ± 2.62, PTX 19.17 ± 3.551, PTX and AFC-5128 24.94 ± 4.708; burst duration ([F(2,11) = 1.327; $p = 0.2857$)]: baseline 1025 ± 202.9, PTX 1209 ± 220.7, PTX and AFC-5128 1367 ± 299.5 ms) and interburst interval ([F(2,11) = 1.365; $p = 0.2725$)]: baseline 20701 ± 5737, PTX 12334 ± 2778, PTX and AFC-5128 17696 ± 4797 ms) (Figure 4b-e). Similar results were observed with the P2X7R antagonist JNJ-47965567. Comparison of burst parameters during PTX application vs. co-application of PTX and JNJ-47965567 revealed no significant difference in burst frequency ([F(2,6) = 0.1479; p=0.4297)]: baseline 0.0477 ± 0.01258, PTX 0.0692 ± 0.01705, PTX and JNJ-47965567 0.06347 ± 0.02547 Hz), number of spikes in burst ([F(2,6) = 1.696; $p = 0.2322$)]: baseline 31.56 ± 8.213, PTX 59.16 ± 22.14, PTX and JNJ-47965567 26.93.3 ± 9.223), burst duration (baseline 1179 ± 272.6, PTX 1562 ± 281.1, PTX and JNJ-47965567 1230 ± 526.2 ms) and interburst interval ([F(2,6) = 1.606; $p = 0.1916$)]: baseline 15.03± 4.294, PTX 10.19 ± 2.126, PTX and JNJ-47965567 19.90± 7.103 s) (Figure 4f-i).

Τηε αβοε φινδινγς ινδιςατε τηατ Π2Ξ7Ρ ανταγονισμ ις νοτ συφφιςιεντ το πρεεντ αςυτε επιλεπτιφορμ-λικε αςτιιτψ εοκεδ βψ ΠΤΞ ιν τηις ηυμαν μοδελ. Ωε ηψποτηεσιζεδ τηις μαψ βεςαυσε οφ τηε αβσενςε οφ ανψ βαςκγρουνδ ινφλαμματορψ τονε. Το τεστ τηις ιδεα, ωε αδαπτεδ τηε μοδελ το μορε ςλοσελψ ρεφλεςτ ςηρονις ινφλαμματορψ ςονδιτιονς

βψ co-treating the PTX-exposed hiPSC-derived neuronal networks with a cocktail of pro-inflammatory agents (TNΦ-α, IΛ-1α, IΛ-1β and ˜1χ) for 7 to 12 days (Figure 4θ). Previous data have shown that treatment with these agents leads to a neuroinflammatory phenotype in hiPSC-derived neuronal networks (Hyvarinen et al., 2019; Stoberl et al., 2023). Loose patch-clamp recordings were performed in the presence of PTX alone or PTX and AFC-5128 from the neuronal cultures treated with PTX and pro-inflammatory agents. In contrast to results from our acute settings, burst frequency was significantly reduced in the presence of AFC-5128 (PTX 0.1012 ± 0.0156, PTX and AFC-5128 0.0662 ± 0.0159 Hz;p = 0.0342) (Figure 4k) illustrating that P2X7R antagonism alleviates hyperexcitability in a chronic model of epileptiform-like events under inflammatory conditions. Moreover, the mean number of spikes in burst (PTX 19.20 ± 2.771, PTX and AFC-5128 14.95 ± 2.542 Hz;p = 0.1688) and burst duration (PTX 1404 ± 274.4, PTX and AFC-5128 1264 ± 209.5 ms; p = 0.1688) were slightly reduced in the presence of AFC-5128, however, this did not reach statistical significance (Figure 4l, m). Finally, mean inter-burst-intervals (IBI) were also increased following AFC-5128 application (PTX 10.61 ± 2.370, PTX and AFC-5128 40.87 ± 16.28 s; p = 0.0479) (Figure 4n).

Next, we used histograms and kernel density plots to delineate IBI subpopulations Figure 4o-q). After the addition of AFC-5128, a distinct peak appeared (indicated by arrow in Figure 4p) at longer IBIs indicating AFC-5128 increases successive intervals between bursts. Furthermore, the shape and scale parameters of the distribution of the IBIs were measured by fitting a gamma distribution to the histogram (Figure 4r, s and Table 1). We found that the mean shape parameter of the gamma distribution of IBI was 0.794 in PTX-treated group and 0.482 in PTX and AFC-5128 co-treated group. Similarly, the mean scale parameter from the gamma distribution was 8.722 in PTX-treated group but increased to 31.048 in PTX and AFC-5128 co-treated group demonstrating increase in longer intervals between bursts when AFC-5128 was co-applied. Comparison of the cumulative frequency distributions of PTX or PTX and AFC-5128 treated groups also revealed increase in IBI after AFC-5128 application (Figure 4t; p = 0.0198). These results provide additional confirmation that AFC-5128 increases the IBI in chronic inflammatory model of epileptiform-like events.

Taken together, while P2X7R antagonism seems to have no effect on acute PTX-induced epileptiform activity, treatment with P2X7R antagonists reduced seizure-like events under chronic inflammatory conditions.

3.3. Synergist effect of P2X7R antagonism in carbamazepine-resistant iPSC-derived neuronal network model of epileptiform-like events

Recent studies showed that blocking the P2X7R attenuates pharmacoresistant status epilepticus in a mouse model (Beamer et al., 2022). We, therefore, hypothesized that P2X7R antagonism may also enhance the effects of conventional ASMs in our in vitro hiPSC-derived neural network model treated with neuroinflammatory agents.

As before, hiPSC-derived neural networks were treated with PTX and the same cocktail of neuroinflammatory agents as before (*i.e.*, TNF-a, IL-1a, IL-1 and C1q) for 7-12 days. Loose patch-clamp experiments were performed in baseline conditions and in the presence of the common ASM carbamazepine (50 µM) (Figure 5a, b). Neurons were categorised as unresponsive to carbamazepine if carbamazepine application failed to reduce firing frequency by more than 30%, leading to 68.8% carbamazepine-unresponsive neurons when co-treated with PTX and neuroinflammatory agents (Figure 5c). Next, we wanted to explore if the P2X7R antagonist AFC-5128 attenuates carbamazepine-resistant epileptiform-like burst firing. Representative traces depicting burst firing indicated attenuation of epileptiform-like activity when the neural network was co-treated with carbamazepine and AFC-5128 (Figure 5d). While the burst frequency did not change significantly in the presence of carbamazepine, this was

reduced to a significant level via the co-application of carbamazepine and AFC-5128 (PTX vs. PTX and CBZ (carbamazepine): 0.1022 ± 0.0156 vs. 0.1187 ± 0.0264 Hz; $p = 0.8666$; PTX and CBZ vs. PTX, CBZ and AFC-5128: 0.1187 ± 0.02645 Hz vs. 0.04713 ± 0.01130 Hz; $p = 0.0442$) (Figure 5e). Interestingly, co-application of carbamazepine and AFC-5128 also led to a reduction in the number of spikes in burst (PTX vs. PTX and CBZ: 27.94 ± 3.583 vs. 15.73 ± 3.678; $p = 0.0173$; PTX and CBZ vs. PTX and CBZ and AFC-5128: 15.73 ± 3.678 vs. 12.71 ± 3.239; $p = 0.0017$) (Figure 5f). Similarly, a reduction in the burst duration was observed after carbamazepine application that was further reduced in the presence of AFC-5128, which was statistically significant compared to the burst duration in the presence of carbamazepine alone ([$F(2,11) = 8.6$; $p = 0.0039$]; PTX vs. PTX and CBZ: 1857 ± 227.1 vs. 1321 ± 241.5 ms; $p = 0.1390$; PTX and CBZ vs. PTX, CBZ and AFC-5128: 1321 ± 241.5 vs. 888.5 ± 125.6 ms; $p = 0.0585$; PTX vs. PTX, CBZ and AFC-5128: 1857 ± 227.1 vs. 888.5 ± 125.6 ms;$p = 0.0098$) (Figure 5g). Moreover, while the IBI was only slightly increased in the presence of carbamazepine, the mean IBI was further increased when carbamazepine and AFC-5128 were co-applied, although not statistically significant ([$F(2,11) = 1.199$, $p = 0.2970$]; PTX vs. PTX and CBZ: 11.06 ± 2.493 vs. 15.19 ± 5.057 s;$p = 0.5748$; PTX and CBZ vs. PTX, CBZ and AFC: 15.19 ± 5.057 vs. 106.4 ± 84.75 s; $p = 0.5526$) (Figure 5h).

To further quantify these observations, histograms were made using log-transformed IBI distributions. The data shows a right-shift in the IBI distribution indicating longer IBI after the co-application of carbamazepine and AFC-5128 (Figure 5i-k). Kernel density estimation (KDE) also reveals a shift towards a longer IBI distribution after co-application of carbamazepine and AFC-5128 (Figure 5l). The shape parameters of the distribution of the IBIs were measured by fitting a gamma distribution to the histogram. The distribution of the IBIs and corresponding gamma-distribution fits are shown in Figure 5m-o. The shape and scale parameter as a measurement of the IBI distribution for PTX or PTX and CBZ or for co-application of PTX, CBZ and AFC-5128 is shown in Table 2. The shape parameter as a measure of the spread of the IBI distribution increased form 10.418 in the presence of PTX and CBZ to 17.847 during the co-application of PTX, carbamazepine and AFC-5128.

In addition, comparison of the cumulative frequency distributions of PTX and CBZ or PTX, CBZ and AFC-5128 treated groups also revealed increase in IBI after AFC-5128 application (Figure 5p;$p = 0.008$).

Thus, P2X7R antagonists enhance anti-seizure effects of this conventional ASM in this human model for drug-refractory epilepsy.

4. Discussion

Here, we show for the first time the anti-epileptic potential of blocking the P2X7R using a human in vitro seizure model that included the key contribution of inflammatory signaling. Notably, P2X7R antagonism restored the anti-seizure effects of the ASM carbamazepine in the chronic hiPSC model, suggesting P2X7R-based treatments as add-on therapy for drug-refractory epilepsy.

A key obstacle hampering the translation of results from pre-clinical disease models into the clinic is the lack of their validation in human model systems. In the epilepsy field, new drug development remains largely reliant on pre-clinical drug screening in animal models (Loscher et al., 2013). Human cell models (e.g., hiPSC) offer a promising tool to bridge the translational gap between animal models and human clinical trials. Here, the P2X7R represents no exception. While several P2X7R antagonists have passed onto the clinical trial stage (e.g., depression (Recourt et al., 2023)), the decision to move P2X7R antagonist towards these trials was most likely based on results from animal studies. A growing body of evidence supports the P2X7R as a drug target for epilepsy but this remains in the pre-clinical domain (Engel, 2023). h iPSCs represent a human disease-relevant cellular model to assess phenotypic alterations and drug responses in neurological diseases including epilepsy (Hirose et al., 2020; Lu et al., 2022).

One of the major findings of our study was that P2X7R antagonism reduces epileptiform activity in hiPSCs. This was, however, only evident when an inflammatory tone was present, evoked by co-culturing with a cocktail of cytokines. These results are in line with previous data suggesting the pro-excitability effects of the P2X7R emerge only in the context of neuroinflammation (Beamer et al., 2022; Smith et al., 2023). The mechanism of how P2X7Rs promote hyperexcitability in our hiPSC model and whether this is mediated via P2X7Rs expressed in neurons remains to be established. For our epileptiform-like activity induction studies, we used co-cultures of iPSC-derived neurons and human primary astrocytes. While our data confirmed functional P2X7R expression on neurons, we have previously shown P2X7Rs to be functional also on iPSC-derived astrocytes (Kesavan et al., 2023). It is well established that astrocytes play an important role during synaptic communication via their interaction with pre- and post-synaptic compartments (*i.e* ., tripartite synapse) *(Halassa et al., 2010). Astrocytes contribute to neurotransmitter release, such as glutamate and GABA (Cuellar-Santoyo et al., 2022), which may contribute to network hyperexcitability (Khan et al., 2019). In this scenario, P2X7Rs on astrocytes and activated during inflammatory conditions, contribute to the activation of astrocytes and the subsequent increase in neurotransmitter release contributing thereby to the observed epileptiform discharges. Thus, blocking P2X7R activity on astrocytes would reduce astrocyte activation, neurotransmitter release and network hyperexcitability. P2X7Rs are, however also expressed on neurons where they have been shown to regulate, upon activation, the release of neurotransmitters such as glutamate and GABA (Alves et al., 2024; Barros-Barbosa et al., 2018; Sperlagh et al., 2002), which potentially also contributes to the observed changes in network hyperexcitability. The most likely scenario is, however, a combination of both astrocyte and neuronal P2X7R-mediate effects and the exact contribution from each cell type should be further investigated in future studies. Why the observed effects are restricted to neuroinflammatory conditions and do not impact on network hyperexcitability in an acute setting is likely due to the need for the P2X7R to be primed, for example via increased inflammation, which is in line with the observed absence on acute seizures in experimental animal models (Dogan et al., 2020; Fischer et al., 2016).*

A second major finding of our study is the fact that P2X7R antagonism restores the anticonvulsive effects of the ASM carbamazepine. We have previously shown increased P2X7R expression to contribute to drug-unresponsiveness during status epilepticus, including the ASM carbamazepine (Beamer et al., 2022). The same study also showed that increased inflammation increases status epilepticus-induced drug-refractoriness, which can be overcome by genetic deletion of the P2X7R or via treatment with P2X7R antagonists (Beamer et al., 2022). Future studies should reveal how P2X7R antagonism under neuroinflammatory conditions restores the anti-convulsant actions of ASMs.

While our study provides the evidence of the anti-seizure potential of P2X7R antagonism in human model systems, there are several shortcomings which should be considered. While our study clearly demonstrates the functional expression of P2X7Rs in neurons, whether there are differences according to neuronal subpopulations has not been addressed and should be carried out in future experiments. As mentioned before, for our hiPSC in vitro model of epileptiform-like events we have used co-cultures of neurons and astrocytes with both cell types expressing P2X7Rs. Moreover, apart from neurons and astrocytes, P2X7Rs are highly expressed in microglia and previous studies have shown P2X7Rs to be expressed also in hiPSC-derived microglia (Francistiova et al., 2021). Future studies should clarify what cell type(s) contribute to P2X7R-mediated hyperexcitability. Our data suggest P2X7R antagonism to restore/potentiate the effects of the ASM carbamazepine. Future studies should establish whether these effects are specific for carbamazepine. Previous studies in animal models of status epilepticus have, however, shown that increased P2X7R expression reduces the responsiveness to several ASMs (*i.e* ., lorazepam, midazolam, carbamazepine and phenytoin) (Beamer et al., 2022).

5. Conclusions

In conclusion, this is the first study providing proof of the anti-epileptic potential of P2X7R antagonism using a human model system and suggests P2X7Rs-based treatments as novel adjunctive therapy for drug-refractory epilepsy.

AUTHOR CONTRIBUTIONS

References

Alves, M., Gil, B., Villegas-Salmeron, J., Salari, V., Martins-Ferreira, R., Arribas Blazquez, M., . . . Engel, T. (2024). Opposing effects of the purinergic P2X7 receptor on seizures in neurons and microglia in male mice. *Brain Behav Immun* . doi:10.1016/j.bbi.2024.05.023Amhaoul, H., Ali, I., Mola, M., Van Eetveldt, A., Szewczyk, K., Missault, S., . . . Dedeurwaerdere, S. (2016). P2X7 receptor antagonism reduces the severity of spontaneous seizures in a chronic model of temporal lobe epilepsy.*Neuropharmacology, 105* , 175-185. doi:10.1016/j.neuropharm.2016.01.018Amorim, R. P., Araujo, M. G. L., Valero, J., Lopes-Cendes, I., Pascoal, V. D. B., Malva, J. O., & da Silva Fernandes, M. J. (2017). Silencing of P2X7R by RNA interference in the hippocampus can attenuate morphological and behavioral impact of pilocarpine-induced epilepsy. *Purinergic Signal, 13* (4), 467-478. doi:10.1007/s11302-017-9573-4Andrejew, R., Oliveira-Giacomelli, A., Ribeiro, D. E., Glaser, T., Arnaud-Sampaio, V. F., Lameu, C., & Ulrich, H. (2020). The P2X7 Receptor: Central Hub of Brain Diseases. *Front Mol Neurosci, 13* , 124. doi:10.3389/fnmol.2020.00124Aronica, E., Bauer, S., Bozzi, Y., Caleo, M., Dingledine, R., Gorter, J. A., . . . Kaminski, R. M. (2017). Neuroinflammatory targets and treatments for epilepsy validated in experimental models. *Epilepsia, 58 Suppl 3* (Suppl 3), 27-38. doi:10.1111/epi.13783Autar, K., Guo, X., Rumsey, J. W., Long, C. J., Akanda, N., Jackson, M., . . . Hickman, J. J. (2022). A functional hiPSC-cortical neuron differentiation and maturation model and its application to neurological disorders. *Stem Cell Reports, 17* (1), 96-109. doi:10.1016/j.stemcr.2021.11.009Barros-Barbosa, A. R., Oliveira, A., Lobo, M. G., Cordeiro, J. M., & Correia-de-Sa, P. (2018). Under stressful conditions activation of the ionotropic P2X7 receptor differentially regulates GABA and glutamate release from nerve terminals of the rat cerebral cortex. *Neurochem Int, 112* , 81-95. doi:10.1016/j.neuint.2017.11.005Beamer, E., Fischer, W., & Engel, T. (2017). The ATP-Gated P2X7 Receptor As a Target for the Treatment of Drug-Resistant Epilepsy. *Front Neurosci, 11* , 21. doi:10.3389/fnins.2017.00021Beamer, E., Kuchukulla, M., Boison, D., & Engel, T. (2021). ATP and adenosine-Two players in the control of seizures and epilepsy development. *Prog Neurobiol, 204* , 102105. doi:10.1016/j.pneurobio.2021.102105Beamer, E., Morgan, J., Alves, M., Menendez Mendez, A., Morris, G., Zimmer, B., . . . Engel, T. (2022). Increased expression of the ATP-gated P2X7 receptor reduces responsiveness to anti-convulsants during status epilepticus in mice.*Br J Pharmacol, 179* (12), 2986-3006. doi:10.1111/bph.15785Cuellar-Santoyo, A. O., Ruiz-Rodriguez, V. M., Mares-Barbosa, T. B., Patron-Soberano, A., Howe, A. G., Portales-Perez, D. P., . . . Estrada-Sanchez, A. M. (2022). Revealing the contribution of astrocytes to glutamatergic neuronal transmission. *Front Cell Neurosci, 16* , 1037641. doi:10.3389/fncel.2022.1037641Devinsky, O., Vezzani, A., Najjar, S., De Lanerolle, N. C., & Rogawski, M. A. (2013). Glia and epilepsy: excitability and inflammation. *Trends Neurosci, 36* (3), 174-184. doi:10.1016/j.tins.2012.11.008Dogan, E., Aygun, H., Arslan, G., Rzayev, E., Avci, B., Ayyildiz, M., & Agar, E. (2020). The Role of NMDA Receptors in the Effect of Purinergic P2X7 Receptor on Spontaneous Seizure Activity in WAG/Rij Rats With Genetic Absence Epilepsy. *Front Neurosci, 14* , 414. doi:10.3389/fnins.2020.00414Dona, F., Ulrich, H., Persike, D. S., Conceicao, I. M., Blini, J. P., Cavalheiro, E. A., & Fernandes, M. J. (2009). Alteration of purinergic P2X4 and P2X7 receptor expression in rats with temporal-lobe epilepsy induced by pilocarpine. *Epilepsy Res, 83* (2-3), 157-167. doi:10.1016/j.eplepsyres.2008.10.008Donnelly-Roberts, D. L., Namovic, M. T., Han, P., & Jarvis, M. F. (2009). Mammalian P2X7 receptor pharmacology: comparison of recombinant mouse, rat and human P2X7 receptors. *Br J Pharmacol, 157* (7), 1203-1214. doi:10.1111/j.1476-5381.2009.00233.xEngel, T. (2023). The P2X7 Receptor as a Mechanistic Biomarker for Epilepsy. *Int J Mol Sci, 24* (6). doi:10.3390/ijms24065410Engel, T., Gomez-Villafuertes, R., Tanaka, K., Mesuret, G., Sanz-Rodriguez, A., Garcia-Huerta, P., . . . Diaz-Hernandez, M. (2012). Seizure suppression and neuroprotection by targeting the purinergic P2X7 receptor during status epilepticus in mice. *FASEB J, 26* (4), 1616-1628. doi:10.1096/fj.11-196089Engel, T., Smith, J., & Alves, M. (2021). Targeting Neuroinflammation via Purinergic P2 Receptors for Disease Modification in Drug-Refractory Epilepsy. *J Inflamm Res, 14* , 3367-3392. doi:10.2147/JIR.S287740Fischer, W., Franke, H., Krugel, U., Muller, H., Dinkel, K., Lord, B., . . . Engel, T. (2016). Critical Evaluation of P2X7 Receptor Antagonists in Selected Seizure Models. *PLoS One, 11* (6), e0156468. doi:10.1371/journal.pone.0156468Francistiova, L., Voros, K., Lovasz, Z., Dinnyes, A., & Ko-

bolak, J. (2021). Detection and Functional Evaluation of the P2X7 Receptor in hiPSC Derived Neurons and Microglia-Like Cells. *Front Mol Neurosci, 14* , 793769. doi:10.3389/fnmol.2021.793769Halassa, M. M., & Haydon, P. G. (2010). Integrated brain circuits: astrocytic networks modulate neuronal activity and behavior. *Annu Rev Physiol, 72* , 335-355. doi:10.1146/annurev-physiol-021909-135843Hedegaard, A., Monzon-Sandoval, J., Newey, S. E., Whiteley, E. S., Webber, C., & Akerman, C. J. (2020). Pro-maturational Effects of Human iPSC-Derived Cortical Astrocytes upon iPSC-Derived Cortical Neurons. *Stem Cell Reports, 15* (1), 38-51. doi:10.1016/j.stemcr.2020.05.003Hirose, S., Tanaka, Y., Shibata, M., Kimura, Y., Ishikawa, M., Higurashi, N., . . . Ishii, A. (2020). Application of induced pluripotent stem cells in epilepsy. *Mol Cell Neurosci, 108* , 103535. doi:10.1016/j.mcn.2020.103535Hyvarinen, T., Hagman, S., Ristola, M., Sukki, L., Veijula, K., Kreutzer, J., . . . Narkilahti, S. (2019). Co-stimulation with IL-1beta and TNF-alpha induces an inflammatory reactive astrocyte phenotype with neurosupportive characteristics in a human pluripotent stem cell model system. *Sci Rep, 9* (1), 16944. doi:10.1038/s41598-019-53414-9Illes, P., Khan, T. M., & Rubini, P. (2017). Neuronal P2X7 Receptors Revisited: Do They Really Exist? *J Neurosci, 37* (30), 7049-7062. doi:10.1523/JNEUROSCI.3103-16.2017Jimenez-Mateos, E. M., Arribas-Blazquez, M., Sanz-Rodriguez, A., Concannon, C., Olivos-Ore, L. A., Reschke, C. R., . . . Engel, T. (2015). microRNA targeting of the P2X7 purinoceptor opposes a contralateral epileptogenic focus in the hippocampus. *Sci Rep, 5* , 17486. doi:10.1038/srep17486Jimenez-Pacheco, A., Diaz-Hernandez, M., Arribas-Blazquez, M., Sanz-Rodriguez, A., Olivos-Ore, L. A., Artalejo, A. R., . . . Henshall, D. C. (2016). Transient P2X7 Receptor Antagonism Produces Lasting Reductions in Spontaneous Seizures and Gliosis in Experimental Temporal Lobe Epilepsy. *J Neurosci, 36* (22), 5920-5932. doi:10.1523/JNEUROSCI.4009-15.2016Jimenez-Pacheco, A., Mesuret, G., Sanz-Rodriguez, A., Tanaka, K., Mooney, C., Conroy, R., . . . Engel, T. (2013). Increased neocortical expression of the P2X7 receptor after status epilepticus and anticonvulsant effect of P2X7 receptor antagonist A-438079. *Epilepsia, 54* (9), 1551-1561. doi:10.1111/epi.12257Johnson, M. A., Weick, J. P., Pearce, R. A., & Zhang, S. C. (2007). Functional neural development from human embryonic stem cells: accelerated synaptic activity via astrocyte coculture.*J Neurosci, 27* (12), 3069-3077. doi:10.1523/JNEUROSCI.4562-06.2007Jones, R. S., da Silva, A. B., Whittaker, R. G., Woodhall, G. L., & Cunningham, M. O. (2016). Human brain slices for epilepsy research: Pitfalls, solutions and future challenges. *J Neurosci Methods, 260* , 221-232. doi:10.1016/j.jneumeth.2015.09.021Kaczmarek-Hajek, K., Zhang, J., Kopp, R., Grosche, A., Rissiek, B., Saul, A., . . . Nicke, A. (2018). Re-evaluation of neuronal P2X7 expression using novel mouse models and a P2X7-specific nanobody. *Elife, 7* . doi:10.7554/eLife.36217Kesavan, J., Watters, O., de Diego-Garcia, L., Mendez, A. M., Alves, M., Dinkel, K., . . . Engel, T. (2023). Functional expression of the ATP-gated P2X7 receptor in human iPSC-derived astrocytes. *Purinergic Signal* . doi:10.1007/s11302-023-09957-8Khan, M. T., Deussing, J., Tang, Y., & Illes, P. (2019). Astrocytic rather than neuronal P2X7 receptors modulate the function of the tri-synaptic network in the rodent hippocampus. *Brain Res Bull, 151* , 164-173. doi:10.1016/j.brainresbull.2018.07.016Klein, P., Dingledine, R., Aronica, E., Bernard, C., Blumcke, I., Boison, D., . . . Loscher, W. (2018). Commonalities in epileptogenic processes from different acute brain insults: Do they translate? *Epilepsia, 59* (1), 37-66. doi:10.1111/epi.13965Klein, P., Kaminski, R. M., Koepp, M., & Loscher, W. (2024). New epilepsy therapies in development. *Nat Rev Drug Discov* . doi:10.1038/s41573-024-00981-wLau, K. E. H., Nguyen, N. T., Kesavan, J. C., Langa, E., Fanning, K., Brennan, G. P., . . . Henshall, D. C. (2024). Differential microRNA editing may drive target pathway switching in human temporal lobe epilepsy. *Brain Commun, 6* (1), fcad355. doi:10.1093/braincomms/fcad355Loscher, W., Klitgaard, H., Twyman, R. E., & Schmidt, D. (2013). New avenues for anti-epileptic drug discovery and development. *Nat Rev Drug Discov, 12* (10), 757-776. doi:10.1038/nrd4126Lu, X., Yang, J., & Xiang, Y. (2022). Modeling human neurodevelopmental diseases with brain organoids.*Cell Regen, 11* (1), 1. doi:10.1186/s13619-021-00103-6Mamad, O., Heiland, M., Lindner, A. U., Hill, T. D. M., Ronroy, R. M., Rentrup, K., . . . Henshall, D. C. (2023). Anti-seizure effects of JNJ-54175446 in the intra-amygdala kainic acid model of drug-resistant temporal lobe epilepsy in mice. *Front Pharmacol, 14* , 1308478. doi:10.3389/fphar.2023.1308478Morgan, J., Alves, M., Conte, G., Menendez-Mendez, A., de Diego-Garcia, L., de Leo, G., . . . Engel, T. (2020). Characterization of the Expression of the ATP-Gated P2X7 Receptor Following Status Epilepticus and during Epilepsy Using a P2X7-EGFP Reporter Mouse. *Neurosci Bull, 36* (11), 1242-1258. doi:10.1007/s12264-020-00573-9Perucca, E., Perucca, P., White, H. S., & Wirrell, E. C. (2023). Drug resistance in epilepsy. *Lancet Neurol, 22* (8), 723-

734. doi:10.1016/S1474-4422(23)00151-5Pitkanen, A., Lukasiuk, K., Dudek, F. E., & Staley, K. J. (2015). Epileptogenesis.*Cold Spring Harb Perspect Med, 5* (10). doi:10.1101/cshperspect.a022822Recourt, K., de Boer, P., van der Ark, P., Benes, H., van Gerven, J. M. A., Ceusters, M., . . . Jacobs, G. E. (2023). Characterization of the central nervous system penetrant and selective purine P2X7 receptor antagonist JNJ-54175446 in patients with major depressive disorder. *Transl Psychiatry, 13* (1), 266. doi:10.1038/s41398-023-02557-5Rivetti di Val Cervo, P., Besusso, D., Conforti, P., & Cattaneo, E. (2021). hiPSCs for predictive modelling of neurodegenerative diseases: dreaming the possible. *Nat Rev Neurol, 17* (6), 381-392. doi:10.1038/s41582-021-00465-0Rozmer, K., Gao, P., Araujo, M. G. L., Khan, M. T., Liu, J., Rong, W., . . . Illes, P. (2017). Pilocarpine-Induced Status Epilepticus Increases the Sensitivity of P2X7 and P2Y1 Receptors to Nucleotides at Neural Progenitor Cells of the Juvenile Rodent Hippocampus. *Cereb Cortex, 27* (7), 3568-3585. doi:10.1093/cercor/bhw178Smith, J., Menendez Mendez, A., Alves, M., Parras, A., Conte, G., Bhattacharya, A., . . . Engel, T. (2023). The P2X7 receptor contributes to seizures and inflammation-driven long-lasting brain hyperexcitability following hypoxia in neonatal mice.*Br J Pharmacol, 180* (13), 1710-1729. doi:10.1111/bph.16033Sperlagh, B., & Illes, P. (2014). P2X7 receptor: an emerging target in central nervous system diseases. *Trends Pharmacol Sci, 35* (10), 537-547. doi:10.1016/j.tips.2014.08.002Sperlagh, B., Kofalvi, A., Deuchars, J., Atkinson, L., Milligan, C. J., Buckley, N. J., & Vizi, E. S. (2002). Involvement of P2X7 receptors in the regulation of neurotransmitter release in the rat hippocampus. *J Neurochem, 81* (6), 1196-1211. doi:10.1046/j.1471-4159.2002.00920.xSteinlein, O. K. (2008). Genetics and epilepsy. *Dialogues Clin Neurosci, 10* (1), 29-38. doi:10.31887/DCNS.2008.10.1/oksteinleinStoberl, N., Maguire, E., Salis, E., Shaw, B., & Hall-Roberts, H. (2023). Human iPSC-derived glia models for the study of neuroinflammation. *J Neuroinflammation, 20* (1), 231. doi:10.1186/s12974-023-02919-2Thijs, R. D., Surges, R., O'Brien, T. J., & Sander, J. W. (2019). Epilepsy in adults. *Lancet, 393* (10172), 689-701. doi:10.1016/S0140-6736(18)32596-0Vezzani, A., French, J., Bartfai, T., & Baram, T. Z. (2011). The role of inflammation in epilepsy. *Nat Rev Neurol, 7* (1), 31-40. doi:10.1038/nrneurol.2010.178

Figure Legends

Φιγυρε 1. *Ιμμυνοφλυορεσχενχε αναλψσις οφ Π2Ξ7Ρς ον ηιΠΣ̃-δεριεδ νευρονς.* ***(α1-α5)*** *Ιμμυνοφλυορεσχενχε αναλψσις οφ ηιΠΣ̃ λινε 1-δεριεδ νευρονς σταινεδ ωιτη αντιβοδιες διρεχτεδ αγαινστ επιτοπε 576-595 οφ ρατ Π2Ξ7Ρς (γρεεν) ωιτη δουβλε-λαβελλινγ υσινγ νευροναλ μαρκερ β-ΙΙΙ τυβυλιν (ρεδ).* ***(β1-β5)*** *Ιμμυνοφλυορεσχενχε αναλψσις οφ ηιΠΣ̃ λινε 2-δεριεδ νευρονς σταινεδ ωιτη αντιβοδιες διρεχτεδ αγαινστ επιτοπε ΑΑ 363 το 595 οφ μουσε Π2Ξ7Ρς (γρεεν) ωιτη δουβλε-λαβελλινγ υσινγ τηε νευροναλ μαρκερ β-ΙΙΙ τυβυλιν (ρεδ).* ***(ς1-ς5)*** *Ιμμυνοφλυορεσχενχε αναλψσις οφ ηιΠΣ̃ λινε 2-δεριεδ νευρονς σταινεδ ωιτη αντιβοδιες διρεχτεδ αγαινστ επιτοπε ΑΑ 576 το ΑΑ 595 (Α1-Α5) οφ ρατ Π2Ξ7Ρς (γρεεν) ωιτη δουβλε-λαβελλινγ υσινγ νευροναλ μαρκερ β-ΙΙΙ τυβυλιν (ρεδ). Σχαλε βαρ 10 μΜ.*

Φιγυρε 2. *ΒζΑΤΠ-εοκεδ $ā^{2+}$ ρεσπονσες ιν ηιΠΣ̃-δεριεδ νευρονς.* ***(α)*** *Αεραγε τιμε σεριες σηοωινγ ρεσπονσε οφ ηιΠΣ̃ λινε 1-δεριεδ νευρονς το τηε απλιχατιον οφ ΒζΑΤΠ (300 μΜ) ιν τηε αβσενχε (βλαχκ τραχε) ανδ πρεσενχε (γρεεν τραχε) οφ ΑΦ̃-5128 (30 νΜ) (Μαννν-Ωηιτνεψ Υ τεστ, ****π < 0.0001, ν = 76).* ***(β)*** *Ινδιιδυαλ πεακ ΔΦ/Φ0 αμπλιτυδε δυρινγ ΒζΑΤΠ ορ ΒζΑΤΠ ανδ ΑΦ̃-5128 χο-απλιχατιον (Μαννν-Ωηιτνεψ Υ τεστ, ****π < 0.0001, ν = 73) ανδ* ***(ς)*** *ΑΥ̃ δυρινγ ΒζΑΤΠ ορ ΒζΑΤΠ ανδ ΑΦ̃-5128 χο-απλιχατιον (Μαννν-Ωηιτνεψ Υ τεστ, ****π < 0.0001, ν = 73).* ***(δ)*** *Ρεσπονσε το ΒζΑΤΠ απλιχατιον ιν ηιΠΣ̃ λινε 1-δεριεδ νευρονς ιν τηε αβσενχε (βλαχκ τραχε) ανδ πρεσενχε (πυρπλε τραχε) οφ ΘΝΘ-47965567. (Μαννν-Ωηιτνεψ Υ τεστ, ****π < 0.0001, ν = 86).* ***(ε)*** *Ινδιιδυαλ πεακ ΔΦ/Φ0 αμπλιτυδε δυρινγ ΒζΑΤΠ ορ ΒζΑΤΠ ανδ ΘΝΘ-47965567 χο-απλιχατιον (Μαννν-Ωηιτνεψ Υ τεστ, ****π < 0.0001, ν = 86) ανδ* ***(φ)*** *ΑΥ̃ δυρινγ ΒζΑΤΠ ορ ΒζΑΤΠ ανδ ΘΝΘ-47965567 χο-απλιχατιον (Μαννν-Ωηιτνεψ Υ τεστ, ****π < 0.0001, ν = 86).* ***(γ)*** *Αεραγε τιμε σεριες σηοωινγ ρεσπονσε οφ ηιΠΣ̃ λινε 2-δεριεδ νευρονς το τηε απλιχατιον οφ ΒζΑΤΠ (300 μΜ) ιν τηε αβσενχε (βλαχκ τραχε) ορ πρεσενχε (γρεεν τραχε) οφ ΑΦ̃-5128 (30 νΜ) (Μαννν-Ωηιτνεψ Υ τεστ, ***π < 0.0001, ν = 57).* ***(η)****Ινδιιδυαλ πεακ ΔΦ/Φ0 αμπλιτυδε δυρινγ ΒζΑΤΠ ορ ΒζΑΤΠ ανδ ΑΦ̃-5128 χο-απλιχατιον (Μαννν-Ωηιτνεψ Υ τεστ, ***π = 0.0111, ν = 52) ανδ****(ι)* *ΑΥ̃ δυρινγ ΒζΑΤΠ ορ ΒζΑΤΠ ανδ ΑΦ̃-5128 χο-απλιχατιον (Μαννν-Ωηιτνεψ Υ τεστ, ***π = 0.0007, ν = 52).* ***(θ)*** *Ρεσπονσε το ΒζΑΤΠ απλιχατιον ιν ηιΠΣ̃ λινε 2-δεριεδ νευρονς ιν τηε αβσενχε (βλαχκ τραχε) ανδ πρεσενχε (πυρπλε τραχε) οφ ΘΝΘ-47965567. (Μαννν-Ωηιτνεψ Υ τεστ, ****π = 0.0002, ν = 26).* ***(κ)*** *Ινδιιδυαλ πεακ ΔΦ/Φ0 αμπλιτυδε δυρινγ ΒζΑΤΠ ορ ΒζΑΤΠ ανδ ΘΝΘ-47965567 χο-απλιχατιον*

*(Μαννϖηιτνεψ Υ τεστ, ****π = 0.0002, ν = 26) ανδ* **(λ)** *ΑΥ˜ δυρινγ ΒζΑΤΠ ορ ΒζΑΤΠ ανδ ΘΝΘ-47965567 σο-αππλιςατιον (Μαννϖηιτνεψ Υ τεστ, ****π = 0.0002, ν = 26).*

Φιγυρε 3. *ηιΠΣ˜-δεριεδ νευροναλ ΠΤΞ μοδελ οφ επιλεπτιφορμ-λικε εεντς ιν ιτρο. (**α**) Σχηεματις ιεω οφ εξπεριμενταλ δεσιγν φορ ασυτε επιλεπτιφορμ-λικε αστιιτψ μοδελ. Αφτερ λοοσε-πατςη ρεςορδινγ ιν βασελινε σονδιτιονς, συσταινεδ επιλεπτιφορμ-λικε αστιιτψ ωας ινδυςεδ βψ 10 μιν εξποσυρε το 100 μΜ ΠΤΞ. Λοοσε πατςηςλαμπ ρεςορδινγς ωερε σοντινυεδ ιν ΠΤΞ δυρινγ συσταινεδ επιλεπτιφορμ-λικε αστιιτψ. **(β)** Εξεμπλαρψ τρασες οφ λοοσε-πατςη ρεςορδινγ σηοωινγ ΠΤΞ-ινδυςεδ βυρστινγ αστιιτψ (ρεδ). **(ς)**Εφφεστ οφ ΠΤΞ (100 μΜ) ον βυρστ φρεχυενςψ (Μαννϖηιτνεψ Υ τεστ, *π = **0.0358** , n = 8). **(d)** Synchronization matrix based upon the peaks of the different fluorescence traces in the presence of physiological saline, PTX or TTX (n = 60). **(e)** Raster plot of calcium transients in the presence of physiological saline, PTX or TTX (n = 60).*

Figure 4 *Effect of AFC-5128 on burst parameters in acute or chronic epileptiform-like activity model. (**a**) Schematic showing experimental design for acute epileptiform-like activity model. Loose-patch recordings were performed in the presence of physiological saline, PTX or PTX and P2X7 antagonists AFC-5128 or JNJ-47965567. (**b-e**) Effect of AFC-5128 on burst parameters in acute PTX model of acute epileptiform-like activity. Burst frequency: baseline vs. PTX, p = 0.3074; PTX vs. PTX and AFC-5128, p = 0.4591; baseline vs. PTX and AFC-5128, p > 0.9999; number of spikes in burst: baseline vs. PTX, p > 0.9999; PTX vs. PTX and AFC-5128, p = 0.3074; baseline vs. PTX and AFC-5128, p = 0.4591; burst duration: baseline vs. PTX, p > 0.9999; PTX vs. PTX and AFC-5128, p > 0.9999; baseline vs. PTX and AFC-5128, p > 0.9999; interburst interval: baseline vs. PTX, p = 0.8593; PTX vs. PTX and AFC-5128, p = 0.0990; baseline vs. PTX and AFC-5128, p = 0.8593 (n = 12). Friedman's ANOVA with Dunn's multiple comparisons test. (**f-i**) Effect of JNJ-47965567 on burst parameters in acute PTX model of epileptiform-like activity.* **Burst frequency: baseline vs. PTX, $p > 0.9999$; PTX vs. PTX and JNJ-47965567, $p = 0.7446$; baseline vs. PTX and JNJ-47965567,$p = 0.4467$; number of spikes in burst: baseline vs. PTX, $p= 0.9999$; PTX vs. PTX and JNJ-47965567, $p = 0.0975$; baseline vs. PTX and JNJ-47965567, $p = 0.1841$; burst duration: baseline vs. PTX, $p = 0.1841$; PTX vs. PTX and JNJ-47965567, $p = 0.0975$; baseline vs. PTX and JNJ-47965567, $p > 0.9999$; interburst interval: baseline vs. PTX, $p > 0.9999$; PTX vs. PTX and JNJ-47965567, $p = 0.5443$; baseline vs. PTX and JNJ-47965567, $p = 0.1841$ (n = 7). Friedman's ANOVA with Dunn's multiple comparisons test.** *(**j**) Schematic showing experimental design for chronic epileptiform-like activity model. Neuronal networks were treated with PTX for 2 days followed by treatment with PTX and neuroinflammatory agents for 7-12 days before loose-patch recordings were performed. (**k-n**) Effect of AFC-5128 on burst frequency, spikes per burst, burst duration and IBI in chronic model of epileptiform-like activity. Burst frequency: PTX vs. PTX and AFC-5128, *p = 0.0342; number of spikes in burst: PTX vs. PTX and AFC-5128, p = 0.3054; burst duration: PTX vs. PTX and AFC-5128, p = 0.5879; interburst interval: PTX vs. PTX and AFC-5128, *p = 0.0479 (n = 13), Wilcoxon matched-pairs signed rank test. (**o-p**) Histogram of IBI distribution using log transformed data overlaid with PDF in the presence of PTX or PTX and AFC-5128. Note the appearance of a population of bursts with longer IBI in the presence of AFC-5128 (indicated by arrow). (**q**) KDE estimation indicating the appearance of a peak (indicated by arrow) at longer IBI in the presence of PTX and AFC-5128. (**r-s**) Histograms of IBI distribution in the presence of PTX or PTX and AFC-5128 fitted with a gamma function. (**t**) Cumulative frequency distribution of IBI upon* **PTX or PTX and AFC-5128 treatment. (Kolmogorov–Smirnov test, $**p = 0.0198$, n = 12).**

Φιγυρε 5 *Εφφεστ οφ ΑΦ˜-5128 ον επιλεπτιφορμ-λικε αστιιτψ ιν ˜BZ-ρεσισταντ μοδελ. (**α**) Σχηεματις σηοωινγ εξπεριμενταλ δεσιγν φορ ˜BZ-ρεσισταντ επιλεπτιφορμ-λικε αστιιτψ μοδελ. Νευροναλ νετωορκς ωερε εξποσεδ το 100 μΜ ΠΤΞ φορ 2 δαψς, φολλοωεδ βψ ΠΤΞ ανδ νευροινφλαμματορψ αγεντς φορ 7-12 δαψς βεφορε λοοσε-πατςηςλαμπ ρεςορδινγς ωερε περφορμεδ ιν τηε πρεσενςε οφ ΠΤΞ ορ ΠΤΞ ανδ ˜BZ ορ ΠΤΞ, ˜BZ ανδ ΑΦ˜-5128. **(β)** Εφφεστ οφ βυρστ φρεχυενςψ ιν τηε πρεσενςε οφ ˜BZ (ν = 16). Νευρονς τηατ φαιλεδ το ρεδυςε βυρστ φρεχυενςψ βψ 70% ορ μορε υπον ˜BZ εξποσυρε ωερε γλασσιφιεδ ας ˜BZ-ρεσισταντ. **(ς)**Ηαρτ σηοωινγ περσενταγε οφ ˜BZ-σενσιτιε ορ ρεσισταντ νευρονς (ν = 16).**(δ)** Εξεμπλαρψ τρασες σηοωινγ βυρστινγ αστιιτψ ιν τηε πρεσενςε οφ ΠΤΞ (τοπ), ΠΤΞ ανδ ˜BZ (μιδδλε) ορ ΠΤΞ, ˜BZ ανδ ΑΦ˜ 5128 (βοττομ) ατ ινδιςατεδ ςονςεντρατιονς. **(ε-η)***

Εφφεςτ οφ ςο-αππλιςατιον οφ ΨBZ ανδ ΑΦΨ-5128 ον βυρστ παραμετερς Burst frequency: **PTX vs. PTX and CBZ: $p = 0.8666$; PTX and CBZ vs. PTX, CBZ and AFC-5128: $*p = 0.0442$; spikes in burst: PTX vs. PTX and CBZ: $*p = 0.0173$; PTX vs. PTX and CBZ and AFC-5128: $**p = 0.0017$;** *burst duration:* **PTX vs. PTX and CBZ: $p = 0.1390$; PTX and CBZ vs. PTX, CBZ and AFC-5128:$p = 0.0585$; PTX vs. PTX, CBZ and AFC-5128: $**p = 0.0098$; IBI: PTX vs. PTX and CBZ: $p = 0.5748$; PTX and CBZ vs. PTX, CBZ and AFC, $p = 0.5526$, n = 12, Friedman's ANOVA with Dunn's multiple comparisons test.** ***(i-k)*** *Histogram of IBI distribution using log transformed data overlaid with PDF in the presence of PTX or PTX and CBZ or PTX, CBZ and AFC-5128. Note the appearance of a population of bursts with longer IBI in the presence of AFC-5128 (n = 12).* ***(l)*** *KDE estimation indicating lower density in the prese of PTX, CBZ and AFC-5128 (n = 12).* ***(m-o)*** *IBI distribution in the presence of PTX or PTX and CBZ or PTX, CBZ and AFC-5128 fitted with a gamma function (n = 12).* ***(p)*** *Cumulative frequency distribution of IBI upon* **PTX and CBZ or PTX, CBZ and AFC-5128 treatment. (Kolmogorov-Smirnov test, $**p = 0.008$, n = 12).**

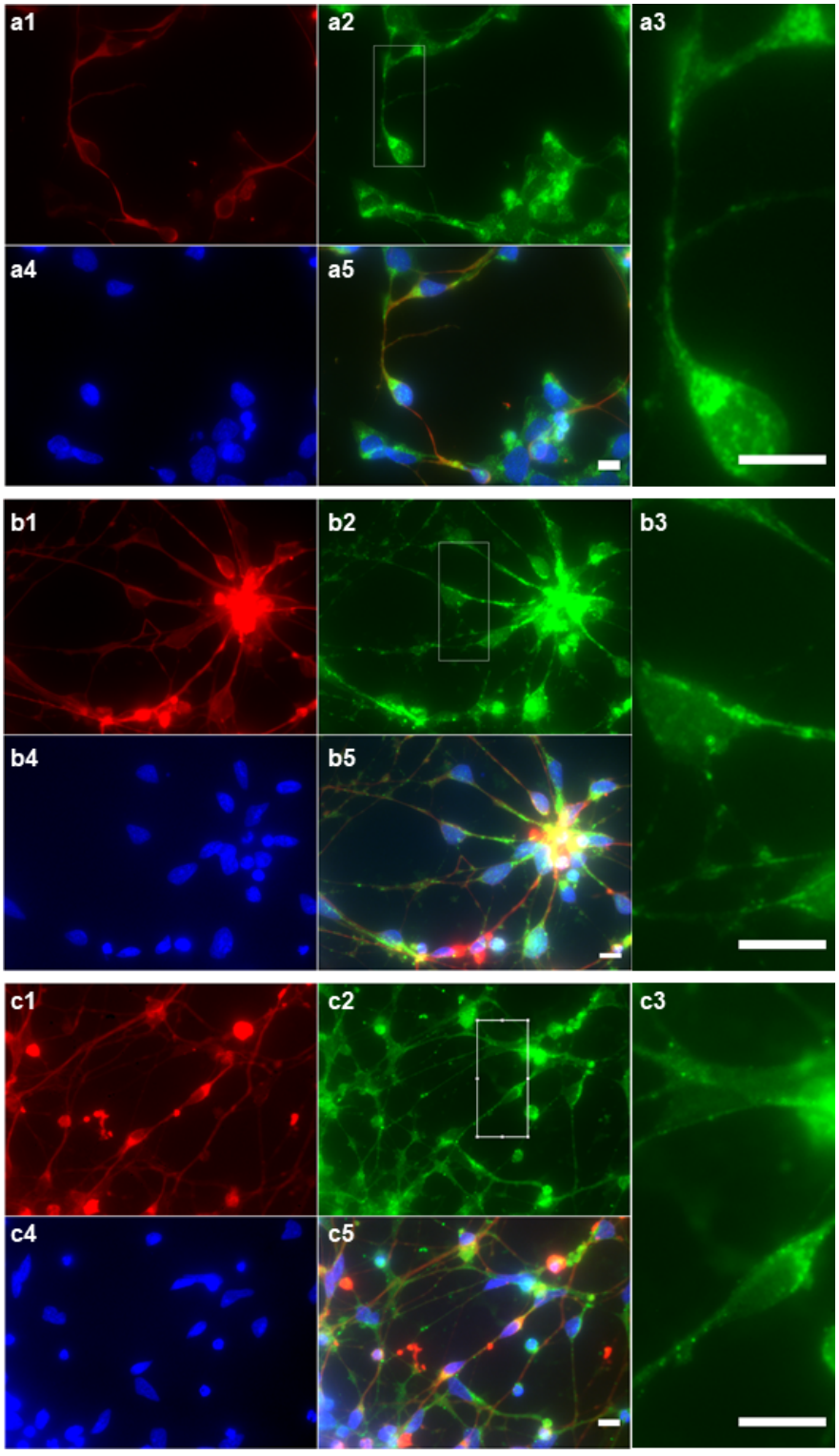

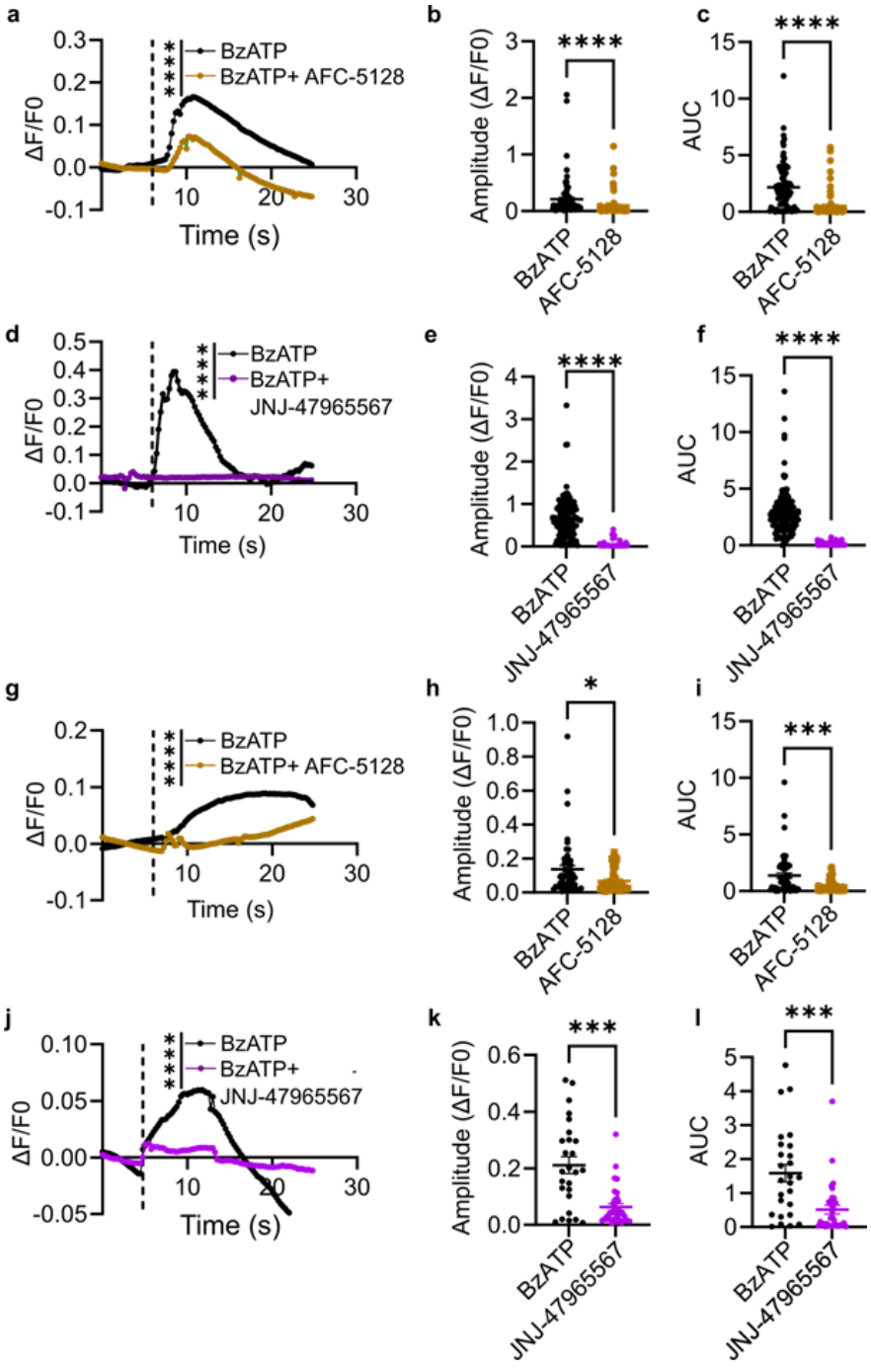

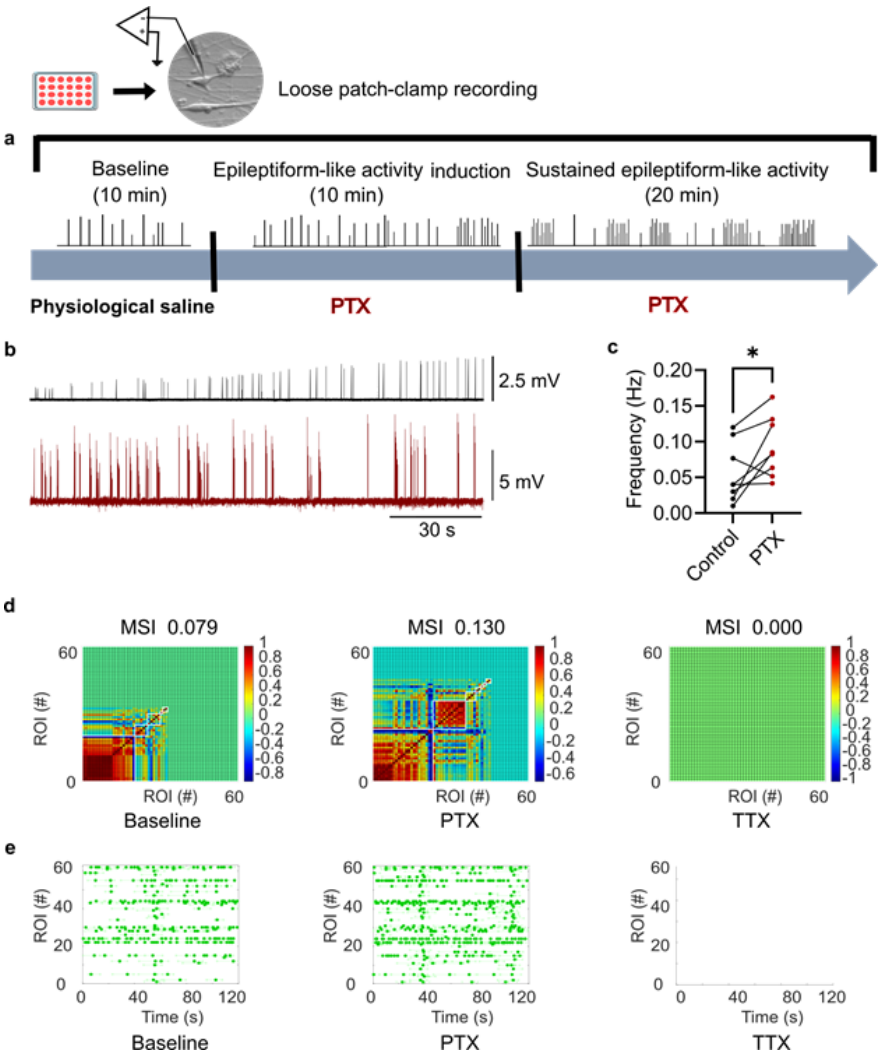

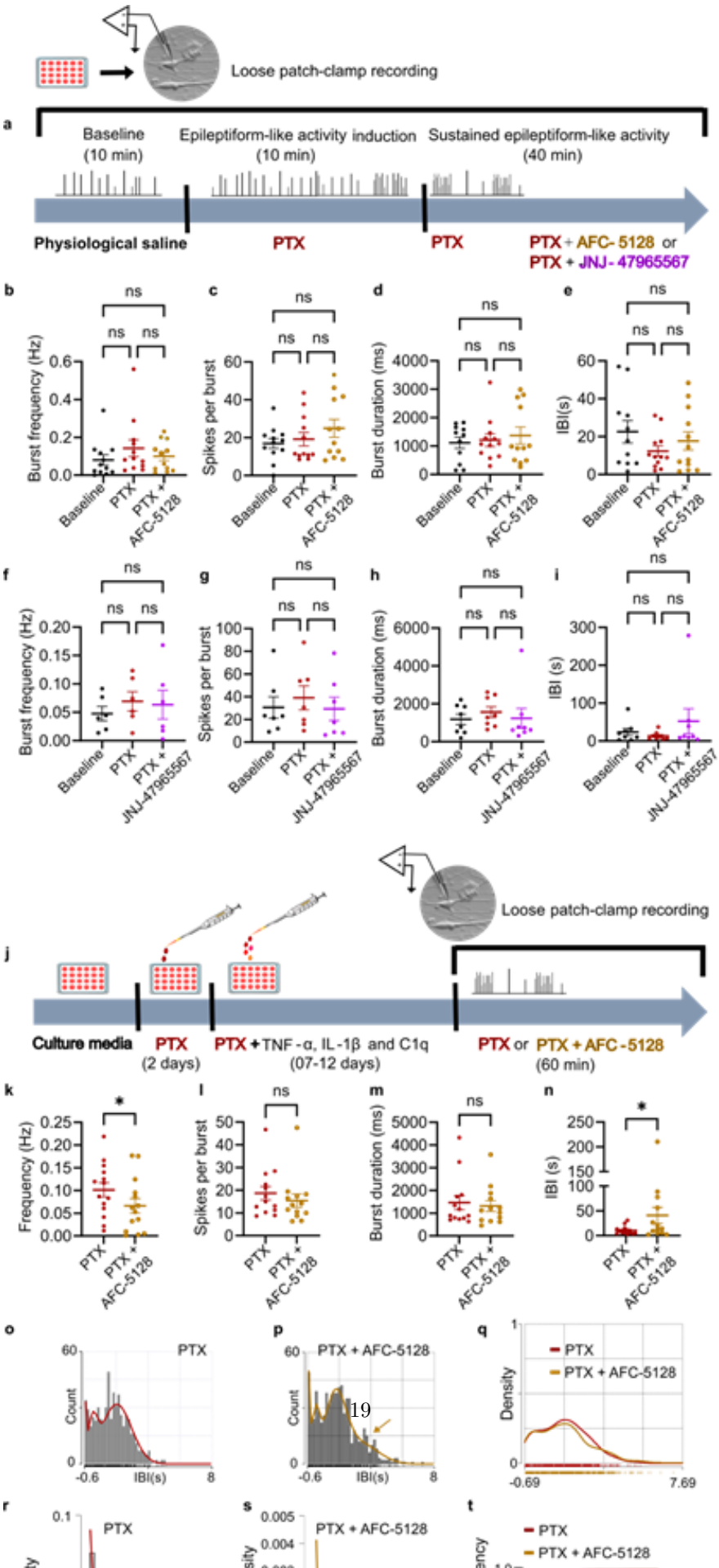

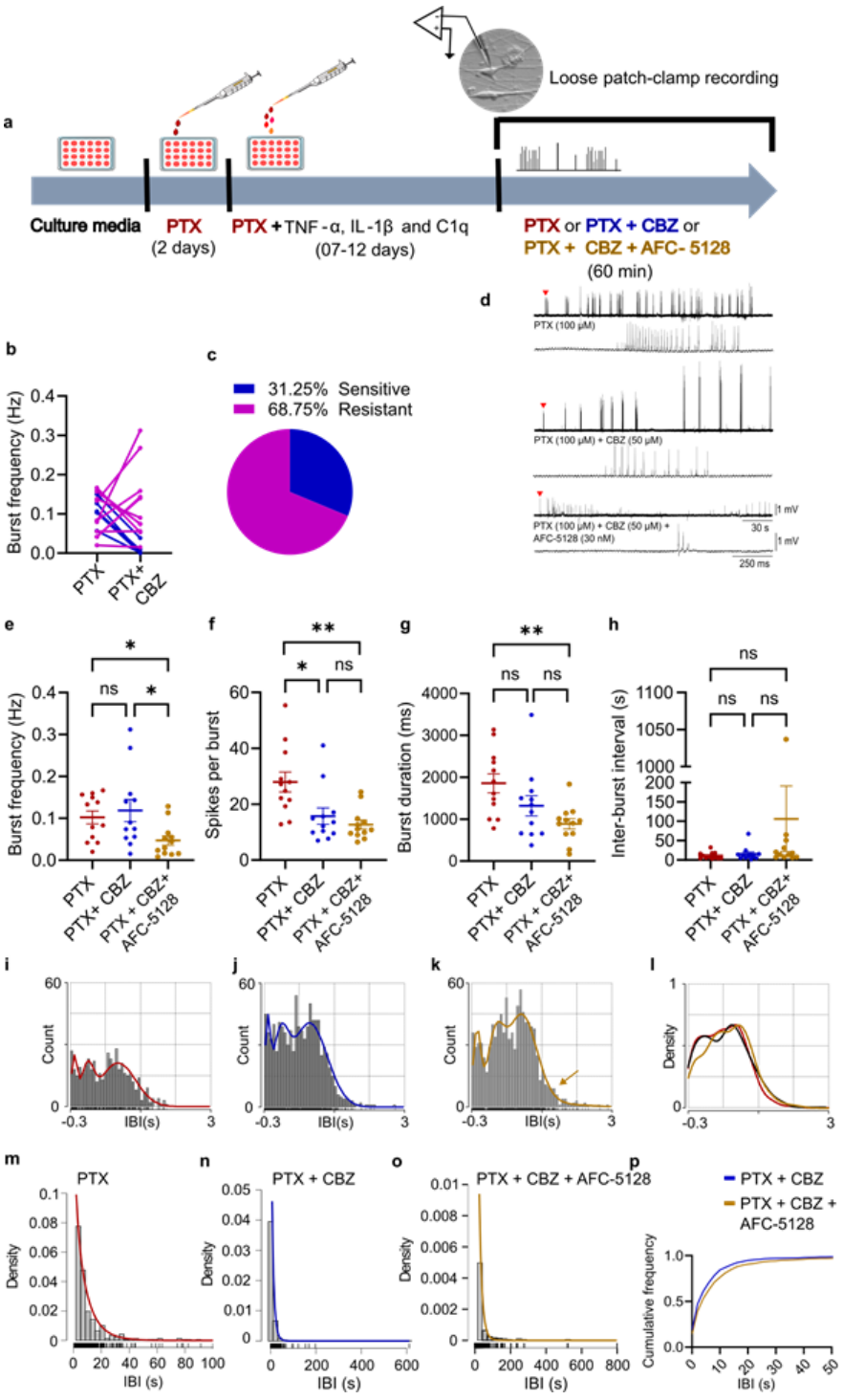

Hosted file

Table 1.docx available at https://authorea.com/users/825726/articles/1221244-p2x7-receptor-antagonism-suppresses-epileptiform-like-activity-in-an-inflammation-primed-human-ipsc-derived-neuron-model-of-drug-resistant-epilepsy

Hosted file

Table 2.docx available at https://authorea.com/users/825726/articles/1221244-p2x7-receptor-antagonism-suppresses-epileptiform-like-activity-in-an-inflammation-primed-human-ipsc-derived-neuron-model-of-drug-resistant-epilepsy